End-to-End Study of the Transfer of Energy from Magnetosheath Ion Precipitation to the Cusp

V. N. Coffey[1], M. O. Chandler[1], Nagendra Singh[2], Levon Avanov[3]

[1]NASA MSFC, [2]UAH, [3]NSSTC,Space Research Institute

The TIDE instrument on Polar often observes evolved ring distributions from magnetic reconnection (Fig. 1). This is a preliminary study of the effects of the unstable magnetosheath distributions on the cusp ionosphere. An end-to-end numerical model was used to study the energy transfer into the high latitude ionosphere based on these solar wind/magnetosheath inputs. This study was addressed in two phases:

1) modeling the evolution of the magnetosheath plasma ring distributions from their injection at the magnetopause to the ionosphere
2) analysis of the wave generation and efficiency of the energy transfer from this magnetosheath precipitation to the near-Earth ionospheric plasma.

The modeling makes use of a semi-kinetic code for plasma transport, and a 2 1/2 D PIC code for wave analysis and energy transfer for an end-to-end impact.

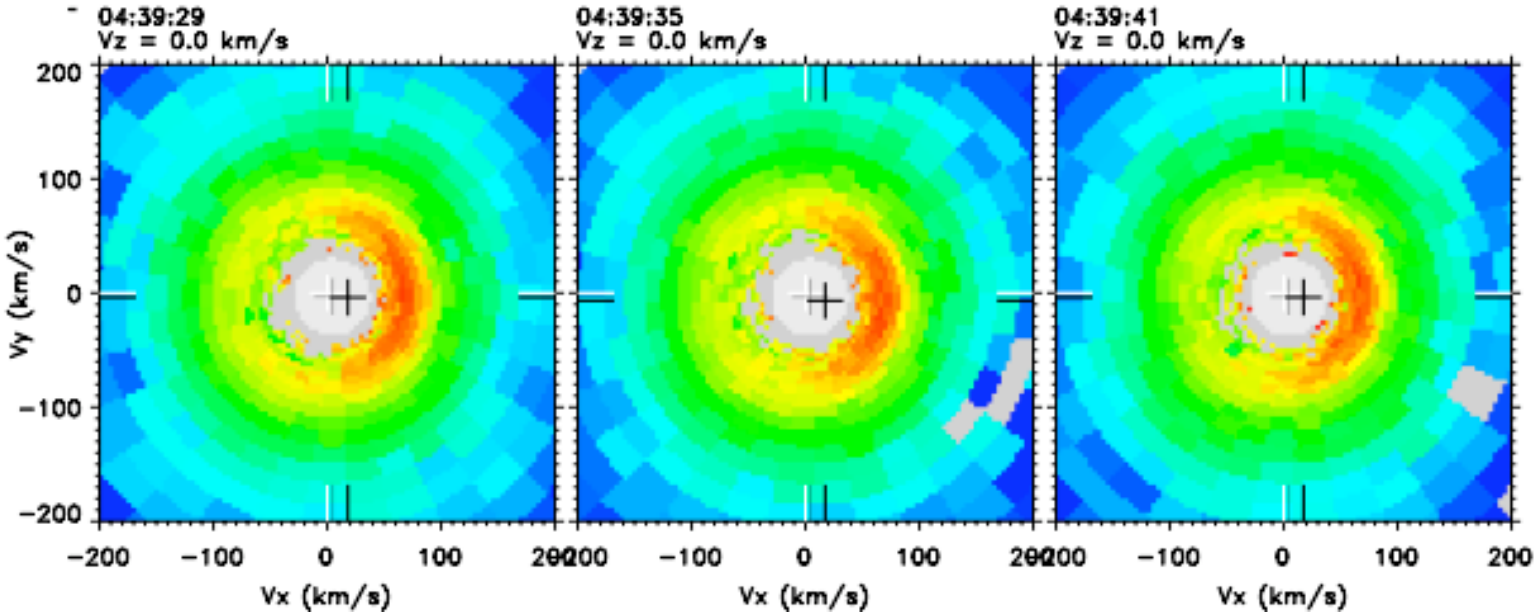

Figure 1. *Observation from the Thermal Ion Dynamics Experiment (TIDE) of ring distributions from magnetosheath precipitation on 4/23/03.*

Model Description, Phase I

- Polar wind initially established in the flux tube
- magnetosheath H^+ injected at the equatorial plane and defined by observed TIDE distribution with:
  - de Hoffman-Teller cut-off at 100 km s^{-1}
  - drift velocity of 200 km s^{-1}
  - parallel and perpendicular temperature of 50 eV and 100 eV. (top left panel page 6)
- used dipolar B and observed B from parameters input into T96 (page 4)

Semi-kinetic code description:

- time-dependent, semi-kinetic plasma model [Wilson, 1990; Singh 1996]
- flux tube defined by the T96 model [Tsyganenko and Stern,1996] starting from 956 km extending to the equatorial magnetopause (See figure 2.)
- includes gravitational force, ambipolar electric field, and magnetic mirror force. Electric field was turned off in these simulations for diagnostic purposes
- H^+, O^+ and neutralizing background of electrons

Model Description, Phase I, Magnetic field configuration

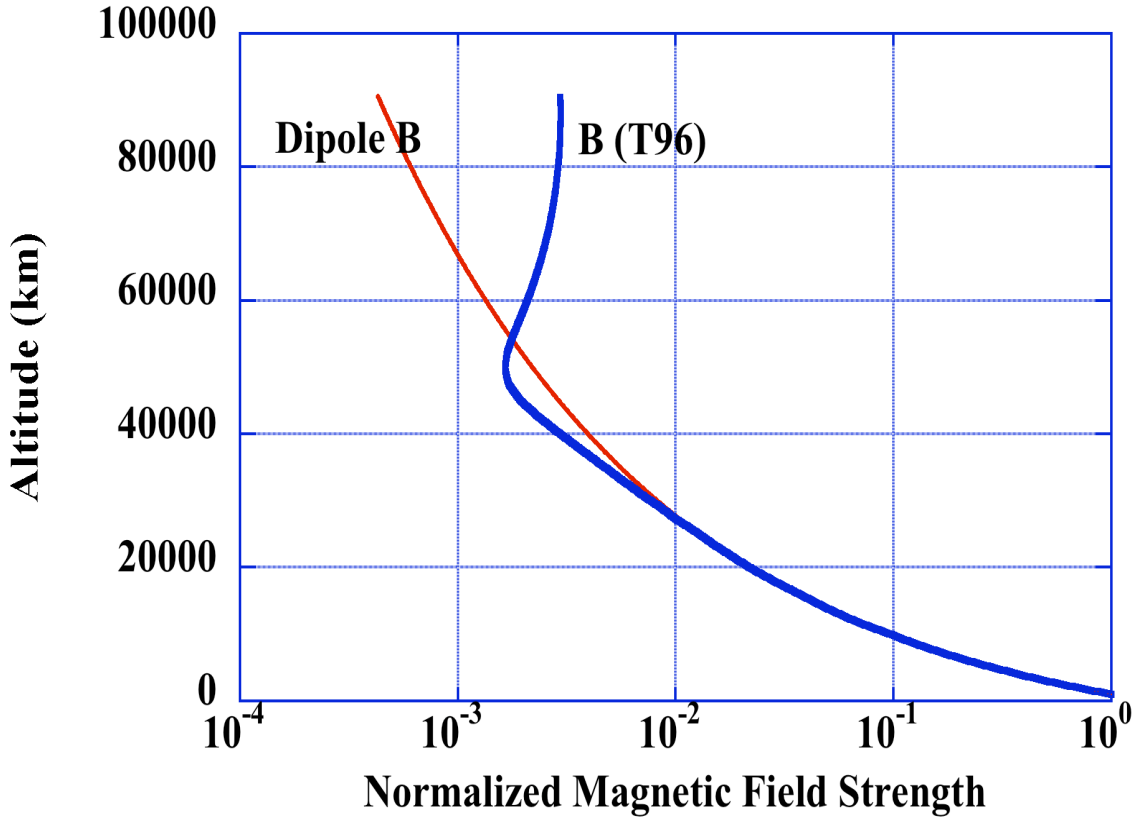

Figure 2. *Configuration of magnetic field strength as a function of altitude used in the simulation runs.*

Results, Phase I

Three types of injections were simulated: single (Fig. 3), pulsed (Fig 4), and continuous (Fig 5).

Each figure consists of 6 panels and includes results from a selected altitude range of the flux tube.

Top left panel shows the initial injected magnetosheath distribution at the top of the flux tube.

The remaining 5 panels from left to right show the evolved distribution within the selected altitude range at different elapsed times in the simulation.

Results, Phase I, Single pulsed injection

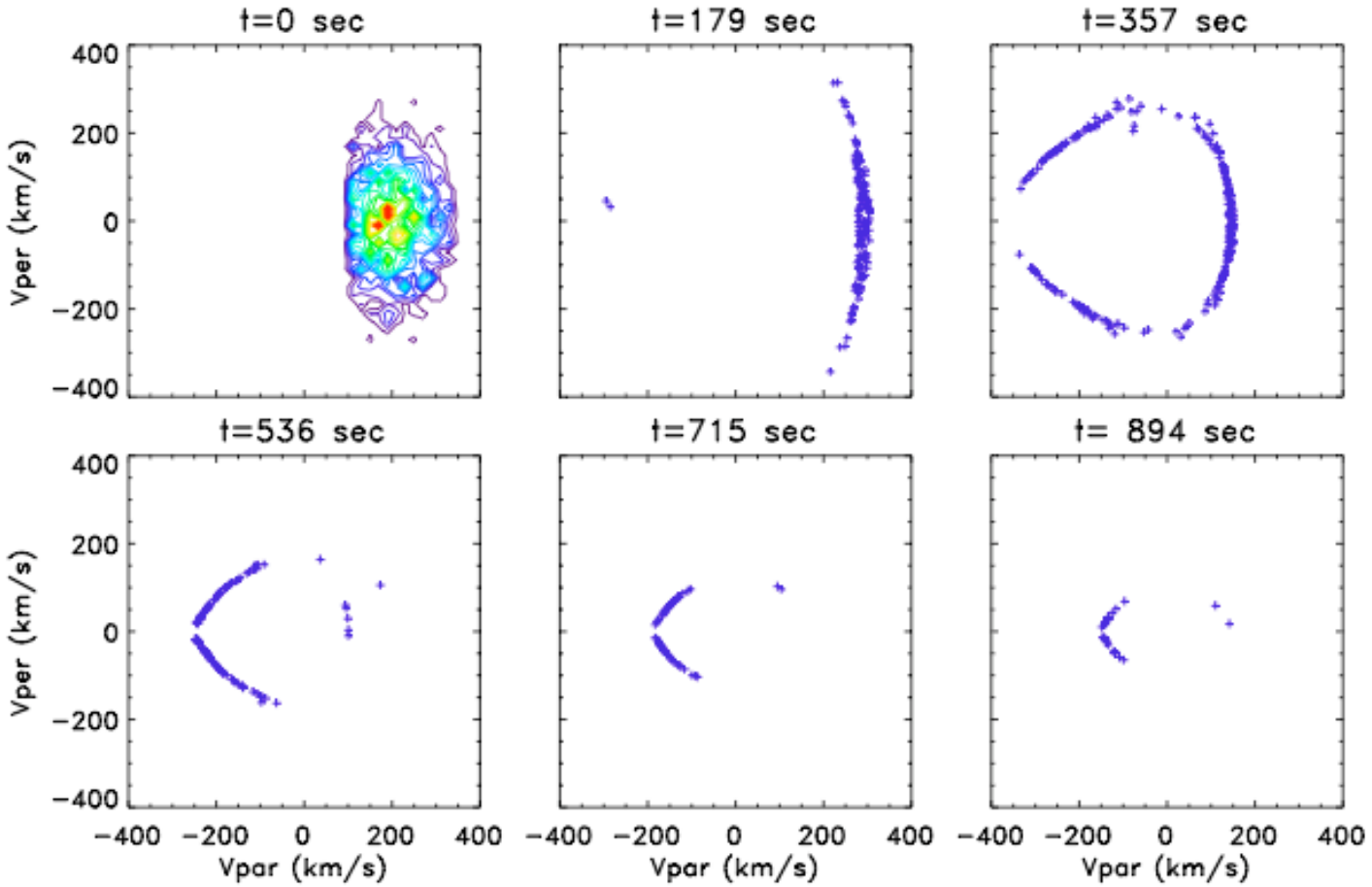

Figure 3. *Results of the injected distribution at 90,408 km and the evolved H^+ velocity distributions from 35000-40000 km from single reconnection simulation.*

Results, Phase I, Continuous injection

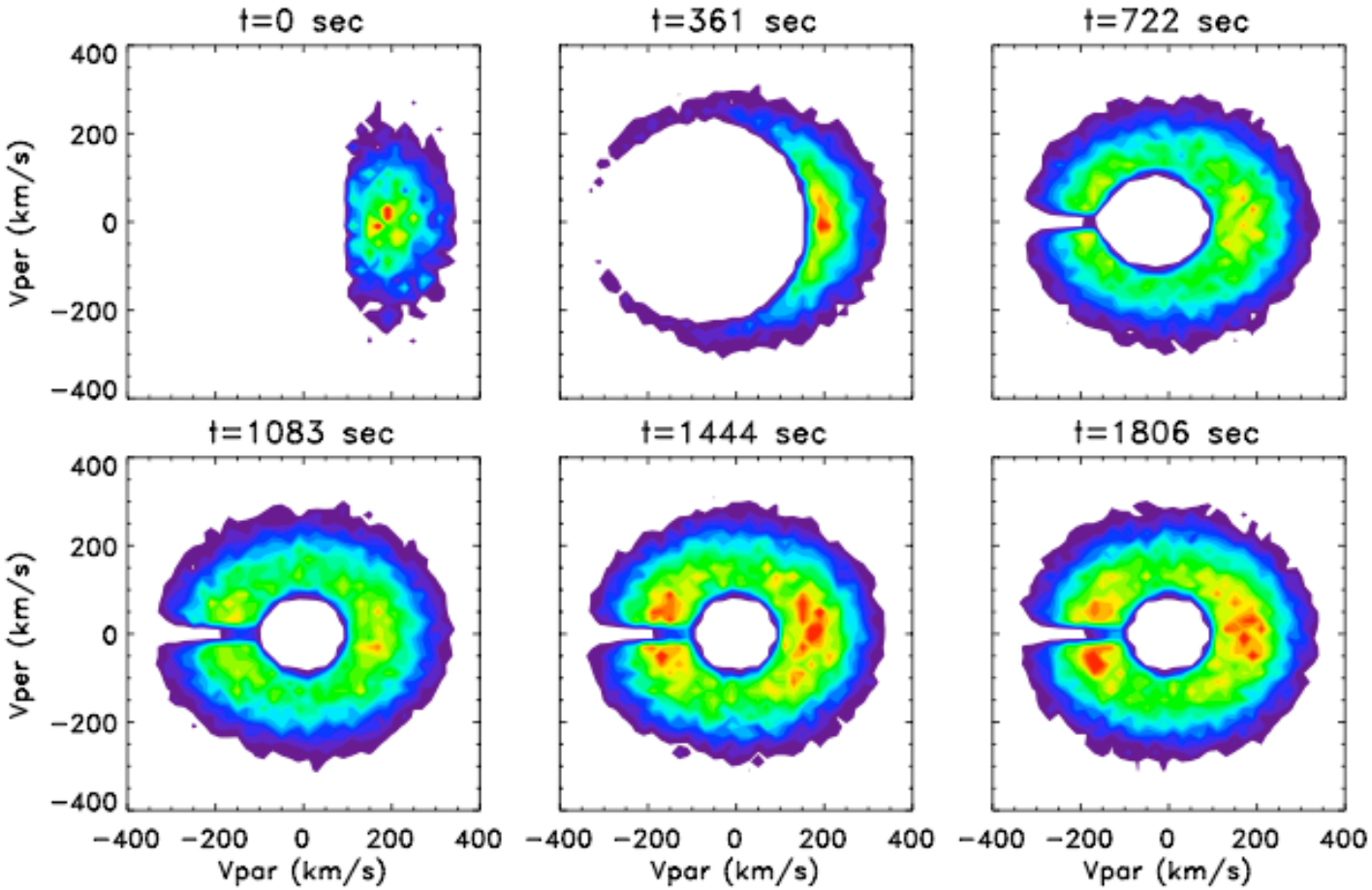

Figure 4. *Results of remotely observed H^+ distributions at 25000-30000 km from continuous reconnection simulation. Note the assymetry in distributions.*

Results, Phase I, Pulsed Injection

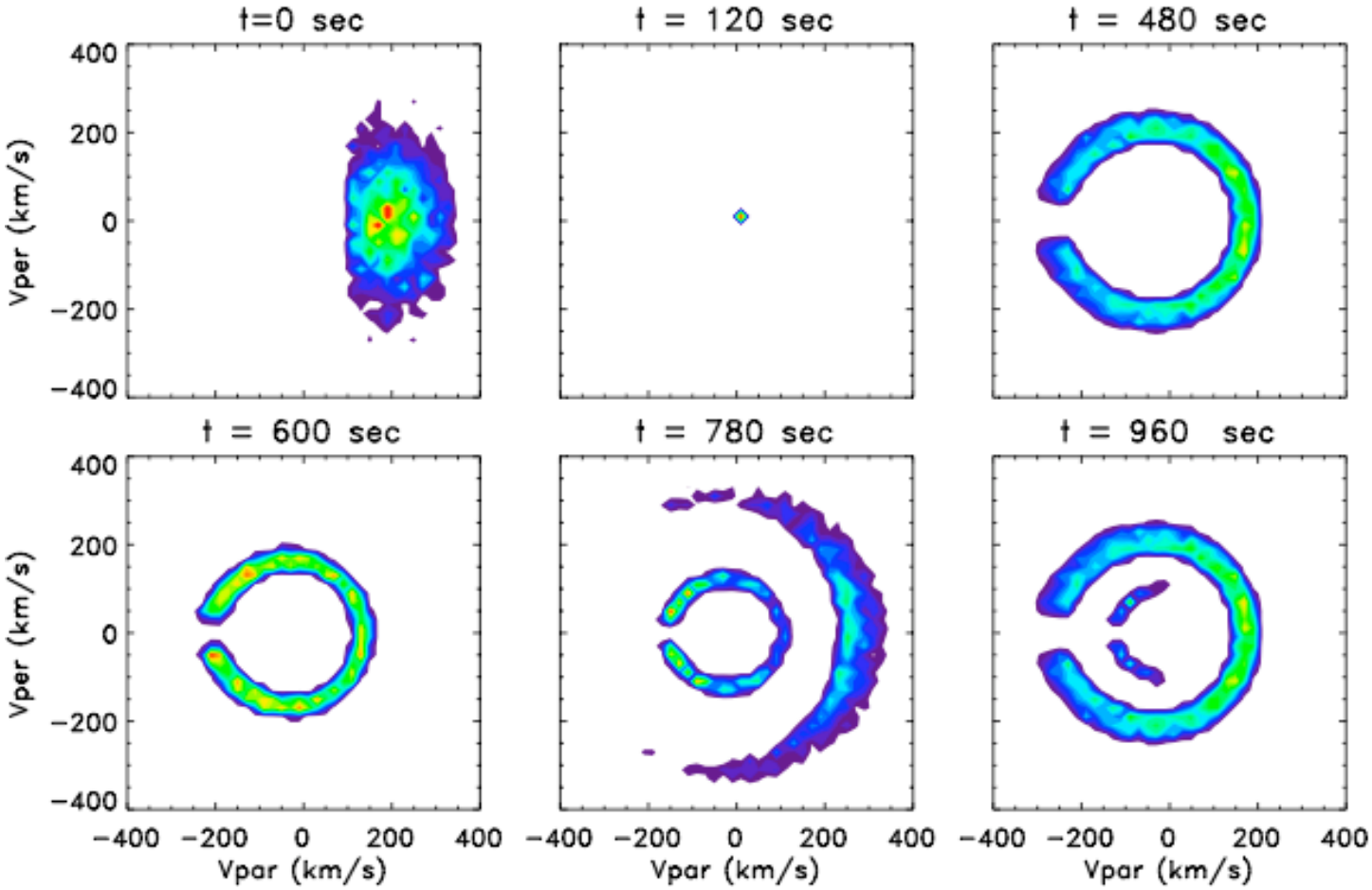

Figure 5. *Results of remotely observed H^+ velocity distributions ranging from 15000-20000 km from pulsed reconnection simulation.*

Model Description, Phase II

The simulated magnetosheath and ionospheric distributions - integrated over the altitude range from 6,000-10,000 km – were used as inputs to a 2 1/2 D PIC code [Singh, 2000] to investigate the efficiency of energy transfer from the precipitating ions to the near-earth ionospheric plasma. The precipitating distribution is evolved and highly non-Maxwellian while the background ionospheric plasma is composed of Maxwellian H^+ and electron distributions with kT=0.3 eV.

2D 1/2 PIC code description and parameters:

- 2D in space and 3D in velocity
- 2D spatial volume is varied by L_x x y_y
  where here L_x=256 λ_d and L_y=128 λ_d
- magnetic field in the x direction
- initial electron and ion temperatures are equal
- magnetosheath and ionospheric density are equal
- ion to electron mass ratio = 1836.

Results, Phase II, Wave generation

Figure 6 shows the power spectrum and wave structure for this simulation as a function of time and shows a fast growing wave in the perpendicular electric field Ey. The initial wave appears to have lasted only a few lower hybrid periods before it decays. The wave frequency peaks near the lower hybrid frequency as shown in the bottom panel.

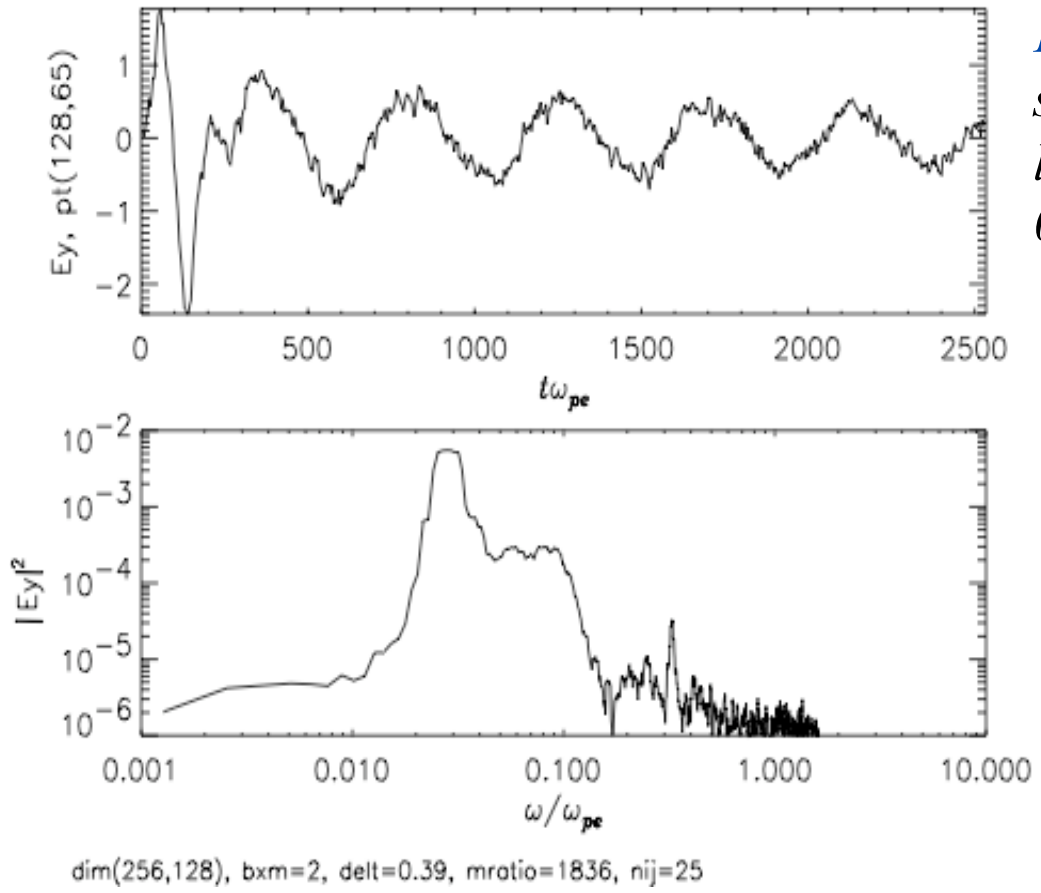

Figure 6. *Electric field and wave spectrum for this simulation. The lower hybrid frequency is near 0.02* ω/ω_{pe}

Results, Phase II, Energy Transfer

Figure 7 shows the resultant energy transfer to the electrons and ions. Electron heating occurs in the parallel direction, consistent with lower hybrid heating. The perpendicular heating of the background H^+ due to the waves is evident where the ratio of Kt_{perp} to $KT_{parallel}$ is 1.33. A simulation with a different magnetosheath distribution yielded a ratio of 1.6.

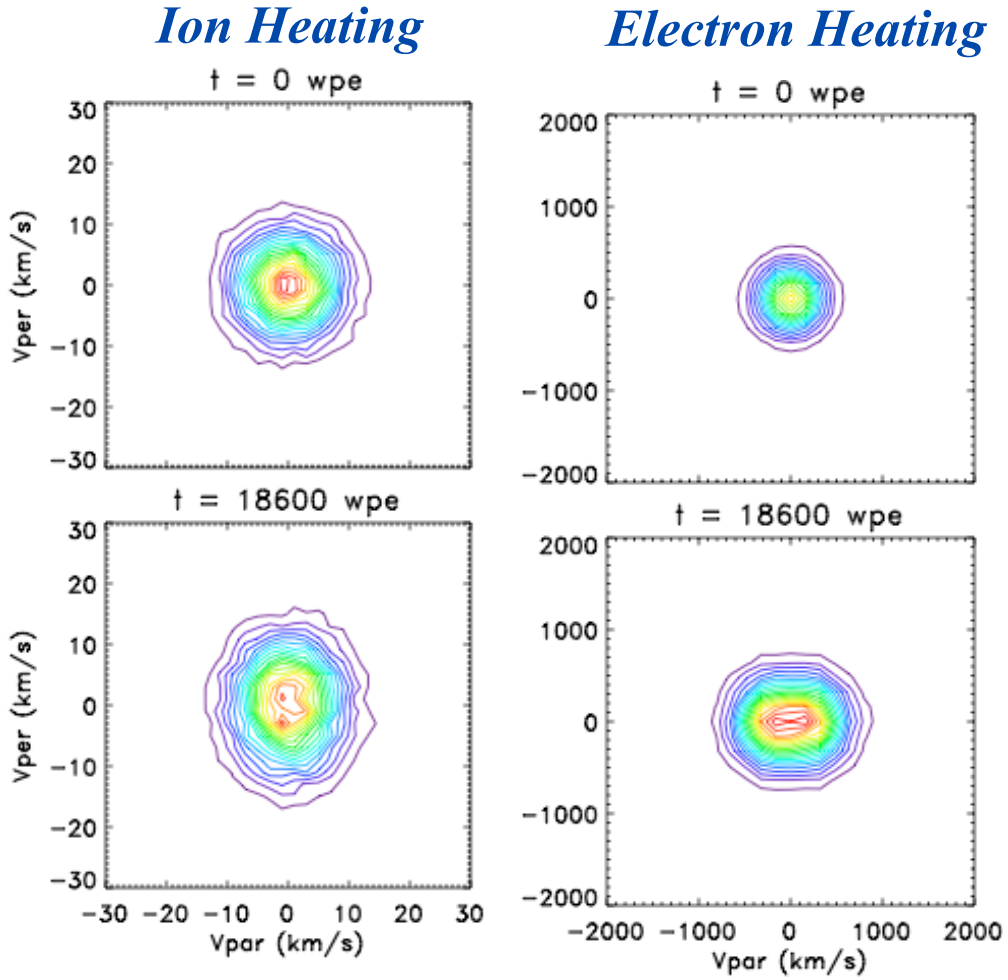

Figure 7. *Distributions of the ambient ionospheric electron and H+ ions a) before and b) after heating by lower hybrid waves. (arbitrary units)*

Conclusion and Future Work

These preliminary results exhibit the type of simulations that can be used for an end-to-end study to interpret the remotely observed distributions from the magnetosheath, the energy transfer to the ionospheric plasma, and the final outflow into the magnetosphere. Future efforts will be in the improvement of the modeling to address the aspects of the different injection scenarios. The resulting ring distributions will then be input for a parameter study in density and mass similar to Roth and Hudson [1985] in their research of lower hybrid heating due to ring distributions. The use of realistic evolved ring distributions will extend their work.

References

Roth, I., M. K. Hudson, Lower Hybrid Heating of Ionospheric Ions Due to Ion Ring Distributions in the Cusp, *J. Geophys. Res.,* Vol. 90. No. A5, p. 4191, 1985.

Singh, N., Time Response of O+ to a Weak Transverse Ion Heating Event in the Polar Ionosphere, *J. Geophys. Res.,* 101, p. 5317, 1996.

Singh, N., Electron holes as a common feature of double-layer driven plasma waves, *Geophys. Res. Lett*, 7, p. 927, 2000.

Tsyganenko, N.A. and D.P. Stern, Modeling the global magnetic field the large-scale Birkeland current systems, J.Geophys.Res., 101, 27187, 1996.

Wilson, G. R. et al.; A New Kinetic Model for Time-Dependent Polar Plasma Outflow: Initial Results, *Geophys. Res. Lett.,* 3, p. 263, 1990.